



**HAL**  
open science

# Turbulent statistical transition from Euler to Lagrange using droplet velocity PDF

J. Anez, R. Canu, Benjamin Duret, J. Reveillon, F.X. X Demoulin

► **To cite this version:**

J. Anez, R. Canu, Benjamin Duret, J. Reveillon, F.X. X Demoulin. Turbulent statistical transition from Euler to Lagrange using droplet velocity PDF. ICLASS 2018 - 14th Triennial International Conference on Liquid Atomization and Spray Systems, Jul 2018, Chicago, United States. hal-02023108

**HAL Id: hal-02023108**

**<https://hal.science/hal-02023108>**

Submitted on 18 Feb 2019

**HAL** is a multi-disciplinary open access archive for the deposit and dissemination of scientific research documents, whether they are published or not. The documents may come from teaching and research institutions in France or abroad, or from public or private research centers.

L'archive ouverte pluridisciplinaire **HAL**, est destinée au dépôt et à la diffusion de documents scientifiques de niveau recherche, publiés ou non, émanant des établissements d'enseignement et de recherche français ou étrangers, des laboratoires publics ou privés.

## Turbulent statistical transition from Euler to Lagrange using droplet velocity PDF

J. J. Anez, R. Canu, B. Duret, J. Reveillon, F.X. Demoulin\*

CNRS CORIA UMR 6614, University of Rouen, Technopole du Madrillet, B.P. 12, 76801  
Saint-Etienne-du-Rouvray Cedex, France

### Abstract

The Euler-Lagrange Spray Atomization model, namely ELSA [18], is a multi-scale approach suitable to perform Large Eddy Simulations (LES) together with the possibility to recover Direct Numerical Simulation (DNS) features for well resolved interfaces. Recent validations with experimental and DNS data were made within the primary break-up [13]. Nevertheless, the link between secondary atomization (where liquid sheets break into ligaments and bag-like structure) and dilute or dispersed zone (where spray of droplets are formed) is still an open question. One of the major challenge within the transition from dense zone (Euler) to dilute zone (Lagrange) is the droplet size and velocity probability density functions (PDF) in turbulent jets. Normally, in diffuse interface models, the averaged mixture velocity and surface interface are employed to set up the lagrangian droplet. Nonetheless, such approach is far from being realistic. Consequently, among novel strategies e.g. 1) local turbulent statistic to improve averaged velocity mixture, 2) Quasi-Multiphase Euler approach [1] to recover averaged velocity in the liquid phase, and 3) local droplet PDF. These techniques will allow a local statistical transition of information from Euler to Lagrange approach. Indeed, an extraction from DNS data has been made, that introduces a new formulation of the drop size distribution (DSD) based on the liquid-gas surface curvature rather than the spherical droplet diameter [3]. The aim of this work is to enhance the coupling Euler-Lagrange in the atomization model, namely ELSA, by including the DSD from DNS approach [3] and velocity PDF from turbulent statistic.

---

### Introduction

For simulation of atomization process, the Eulerian method is used within the secondary and primary atomization. Normally, at the exit of the injector, in order to have a good interface representation, an interface capturing method is used. It allows the representation of complex phenomena and changes on interface topology like breakups or coalescences. However, in the dilute/dispersed zone, the liquid volume fraction is really low and the interface cannot be described accurately even with high resolved DNS, hence some mass conservation problems may arise. An approach used to fix these issues is to couple the Eulerian method with a Lagrangian one, where particle velocities and diameters are obtained from the Eulerian field, and then, Lagrangian information is used to correct the velocity field in the Eulerian transport equations [12].

An Eulerian-Lagrangian hybrid model has also been used in [17]. Where a sub-grid model was performed to take into account the turbulence at unresolved scales. In the sub-grid region near to the interface, a criterion based on energy balance between disruptive and consolidating forces was applied. Hence, a certain number of droplets are created in the corresponding cells. A newer approach is to apply a Droplet Size Distribution (DSD) based on Gauss curvature  $G = \kappa_1 * \kappa_2$  and mean curvature  $H = \frac{\kappa_1 + \kappa_2}{2}$ , which can be defined everywhere from the liquid jet until the dilute zone in order to have a curvature interface evolution during all the atomization process. [3].

Additionally, to appraise Lagrangian droplet trajectory in turbulent liquid jets, some authors have proposed to solve a stochastic differential equation e.g. the Langevin equation. It corresponds to the fundamental principle Newton dynamics with any supplementary force term which corresponds, e.g. the effect of collisions between particles. This force represents a gaussian noise. This type of equation was solved in [4] to have the evolution of distributed particles for the composition PDF method. On this article the governing equations of two-phase flow such as ELSA model are presented and described. These equations are the liquid volume fraction ( $\alpha_l$ ) and liquid/gas interface density  $\Sigma'$  which represents a general term that accounts for all type of ligaments and liquid shapes. And then, a stochastic differential equation derived from the Langevin model for droplets undergoing turbulent dispersion is implemented in OpenFOAM. Moreover, the newly implemented stochastic differential equation is assessed with previous turbulent dispersion model available in OpenFOAM, using experimental and DNS data. Finally, conclusions are drawn from these results in the last section.

\*Corresponding author: demoulin@coria.fr

## Numerical Methods

Turbulence in the carrier fluid implies an unsteady flow field, and in turn unsteady motion of particles, bubbles or drops [7]. Not to mention the significant drag coefficient changes produced by the turbulent motion flow. On the other hand, most of the theory and experiments have been developed for single droplet spheres, only a few have worked in droplet size distribution in liquid jet, e.g.[3, 16]. Interactions of droplets and the formation of clusters with correlated motions play an important role on the hydrodynamic forces exerted by the fluid. Additionally, droplet's motion within this environment will become more costly, computational speaking, as its concentration gets higher. However, on this first research part of the article, the main focus would be the turbulence forces over the cluster of droplet motions in liquid jets.

Modern computational techniques have enabled the coupled use of Finite Element Method (FEM), and the Lattice Boltzmann method (LBM) to observe droplet interactions. In particular, the LBM and its derivative the immersed boundary-lattice Boltzmann method (IB-LBM) is found suitable for droplets of any shapes [10]. On the present article, an Euler-Lagrange Atomization model (ELSA) is used instead. [13, 18]. From this work, different models based on Eulerian modeling for atomization have been studied. Later on, Blokkeel et al. [2] completed the original approach by a Lagrangian description of the spray once the primary break-up is achieved. It is the secondary break-up along with turbulent dispersion applied by the random flow field that is developed on this work.

### *Euler-Lagrange Atomization model (ELSA)*

In ELSA model, the two phases interact through a mixing zone so that both liquid and gas phases coexist with an occupied liquid portion defined by liquid volume fraction ( $\alpha_l$ ). In this context, another approach is included based on a transport equation for the liquid/gas interface density [13, 18]. Moreover, a quasi-multiphase feature has been attached to this approach such as Quasi-Multiphase Euler flow [1] to account for slip velocity between phases and a large eddy simulation (LES) extension has been first carried out by Chesnel et al. [5]. On the present work, the interaction between the phases is made by a single-fluid approach. Therefore, the two-phase flow is studied as a single-fluid turbulent flow composed of two species. Continuity and momentum equations are defined by the known Navier-Stokes equations for incompressible isothermal fluids. Here will be only shown the transport equations for liquid volume fraction ( $\alpha_l$ ), and liquid/gas interface density  $\Sigma'$ , respectively:

$$\begin{cases} \frac{\partial \bar{\alpha}_l}{\partial t} + \nabla \cdot (\bar{U} \bar{\alpha}_l) = -\nabla \cdot \mathbf{R}_{\alpha_l} = \nabla \cdot (\bar{U} \bar{\alpha}_l - \bar{U} \alpha_l) = \nabla \cdot \left( \frac{\nu_t}{Sc_t} \nabla \bar{\alpha}_l \right) \quad , \\ \frac{\partial \bar{\Sigma}'}{\partial t} + \nabla \cdot (\bar{U} \bar{\Sigma}') = \nabla \cdot \left[ \frac{\nu_t}{Sc_t} \nabla \bar{\Sigma}' \right] + C_\Sigma \frac{\Sigma}{\tau_\Sigma} \left( 1 - \frac{\Sigma}{\Sigma^*} \right) \quad . \end{cases} \quad (1)$$

The *turbulent liquid flux*,  $\mathbf{R}_{\alpha_l}$ , appears on the right hand of the first equation from the applied Reynolds-Averaged Navier-Stokes (RANS) filtering procedure, and the two-phase flow decomposition. It represents the transport of the liquid volume fraction induced by velocity fluctuations, and is related to the unresolved part of the velocity that is known to produce additional liquid dispersion. It is to be noted, this formulation is only valid in the absence of slip velocity. Finally,  $\nu_t$  is the turbulent viscosity and  $Sc_t$  is the turbulent Schmidt number, which both being derived from the known Boussinesq's proposal. Regarding the second equation, the interface density  $\Sigma'$ , represents a general variable that accounts for all type of ligaments and liquid shapes. The first term of the right hand side represents the difference between the interface and mixture velocity. It accounts for dispersion of the interface by turbulence. The source term is based on an defined equilibrium value of surface density, namely  $\Sigma^*$ .  $C_\Sigma$  is a constant that is set equal to 0.4. Further details are discussed on [8, 13].

### *Lagrange approach*

Normally, Lagrange interface scale is composed of spherical droplets with no internal momentum, completely isolated from each other within the gaseous atmosphere. For liquid jet atomization, this is far from the truth. For example, Stochastic models based on Kolmogorov analysis, are used for droplet breakup, however, interface dynamics are usually cast aside. Moreover, as previously mentioned, different liquid shapes can be formed at the nearly exit of nozzle injector, which later on, will experience primary and secondary breakups depending on turbulence level [12]. Droplet velocity and position are commonly derived from the known ordinary differential equation (ODE) in which a solid particle drag coefficient is used to calculate the drag force. Nonetheless, in turbulent liquid jets becomes necessary to take into account the so-called *stochastic lagrangian models*.

More than a century ago, Langevin equations were developed as a stochastic model for specific forces on a microscopic droplet undergoing Brownian motion [15, 6]. Therefore, applying the Langevin equation, which is a stochastic differential equation (SDE), the droplet velocity would then follow the paths of Ornstein-Uhlenbeck (OU) processes. This OU process is a statistically stationary Gaussian process completely characterized by its mean, variance and autocorrelation function based on the integral timescale of the process [15]. The SDE based on Langevin equation is as follows:

$$\begin{cases} \frac{d\mathbf{X}^*(t)}{dt} = \mathbf{U}^*(t) \quad , \\ dU_i^*(t) = \frac{-1}{\rho} \frac{\partial \bar{p}}{\partial x_i} dt - \left( \frac{1}{2} + \frac{3C_o}{4} \right) \frac{\epsilon}{\kappa} (U_i^*(t) - \bar{U}_i) dt + (C_o \epsilon)^{1/2} dW_{i(t)} \quad . \end{cases} \quad (2)$$

where  $\mathbf{U}^*(t)$  is the droplet fluctuating velocity with position  $\mathbf{X}^*(t)$ ,  $\mathbf{W}(t)$  is a vector-valued Wiener process. On this work, equation 2 has been implemented to model turbulent dispersion in the software, OpenFOAM [11], and numerically solved using a first-order explicit Euler scheme. Even though higher order schemes are also available from the literature [4], the level of statistical errors arising from the finite number of particles is expected to be minimum. For that purpose, a high amount of particles were injected continuously based on special criteria defined in the following section, until certain statistical sensibility was obtained in the droplet velocity PDF.

### Transition criterion

Eulerian methods are adapted for primary atomization. However, in the dilute zone, the liquid volume fraction is really low and the interface cannot be described accurately even with high resolved simulations like in DNS. An approach used to fix this issue is to couple the Eulerian method with a Lagrangian one. On this article, when the liquid volume fraction is too low to be accurately represented, lagrangian particles are created with a certain diameter, and velocity from the Eulerian field, in order to preserve mass conservation. Then, Lagrangian information is used to correct the velocity field in the Eulerian transport equations. Lagrangian droplets should be initialized taking into account the physics calculated from the Euler field, such as: initial droplet position in the liquid jet, droplet size and velocity distribution. Two criteria are defined for the droplet position:

- *First criteria:  $IRQ_\Sigma$ .* Given by the ratio of the minimum (resolved) interface area,  $\Sigma_{min}$ , over the actual interface area,  $\Sigma$  (eqn. 1). The interface area is more properly defined as "surface area of the liquid-gas interface per unit of volume", defined here as *liquid gas interface density*. And  $\Sigma_{min}$  corresponds to the minimum surface density that can be evaluated for a given value of resolved liquid volume fraction, where "a" is a length scale related to the control volume. Here, a simple approach is used to evaluate  $\Sigma_{min}$ , however, if interface reconstruction were available, the actual resolved interface could be used.  $\Sigma$  follows an additional balance equation as explained in the previous section. Thus, the higher the surface interface fluctuates within a cell, the lower  $IRQ_\Sigma$ , which means subgrid effects become important, and a droplet could be initiated

$$\begin{cases} a\Sigma_{min} = 2.4\sqrt{\alpha_l(1-\alpha_l)} \quad , \\ IRQ_\Sigma = \frac{\Sigma_{min}}{\Sigma} \quad . \end{cases} \quad (3)$$

- *Second criteria:  $IRQ_K$ .* A grid dependant parameter, depending on the actual cell size. Additionally  $IRQ_K$  takes into account the curvature of the interface,  $K$ , defined below. The higher the interface radius, the better the interface resolution, thus less probable to droplet creation. Further discussion on these terms can be found at [12]

$$\begin{cases} K = \nabla \cdot \left( \frac{\nabla \bar{\alpha}_l}{|\nabla \bar{\alpha}_l|} \right) \quad , \\ IRQ_K = \frac{1}{\Delta \cdot K} \quad . \end{cases} \quad (4)$$

- *Third criteria:  $\bar{\alpha}_l$*  It should be clear that droplets should exit only for a low value of liquid volume fraction. The values taken in this work corresponds to the one tabulated in [9] for which was established the presence of droplet for liquid volume fraction below 1% to give the possibility of four and two-way coupling between droplets. Even though in this work only one-way coupling was used in the test case.

## Results and Discussion

The previous section has explained the *stochastic Lagrange model* derived from Langevin equation to account for droplet turbulent dispersion, along with Euler-Lagrange Atomization model (ELSA). Now, an atomization test case is presented. The geometry used in this case is on the left on figure 1, and was selected based on available experimental and DNS results [14, 12]. Moreover, having a low Reynolds and high Weber number, droplet formation and secondary atomization is ensured, as shown on the right of the figure 1 with the radiography spray image:

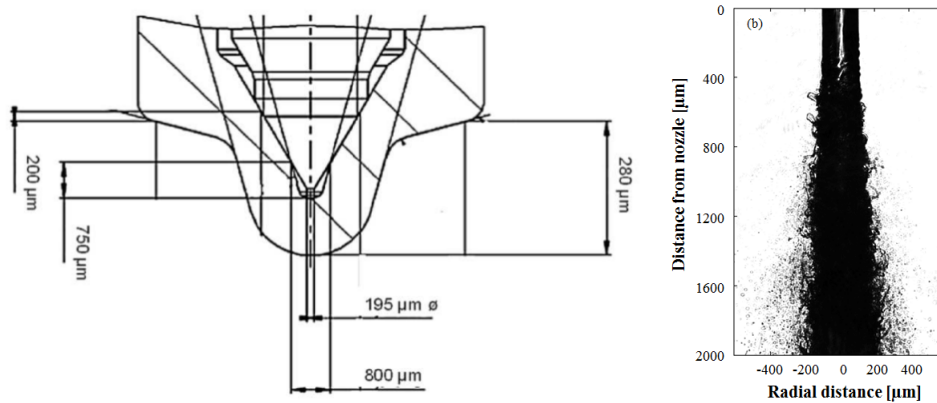


**Figure 1.** Schematic view of the diesel injector nozzle [14].

It is to be noted that the inlet liquid velocity profile was taken from a previous DNS simulation [14], which used a turbulent length scale and intensity of 8%, and 5%, respectively, with atmospheric conditions for the ambient gas pressure. Physical properties are displayed in the table 1.

**Table 1.** Physical properties of Shell NormalFluid ISO 4113 [14, 12].

	Symbols	Value
Liquid Density	$\rho(kg.m^{-3})$	821
Liquid Viscosity	$\mu_l(kg.m^{-1}.s^{-1})$	$3.2 \times 10^{-3}$
Surface tension	$\sigma(N.m^{-1})$	$2.54 \times 10^{-2}$

Finally, experimental interface velocities will be compared against the proposed model radially, on the plane highlighted in red as shown on the figure 2, at 1.5 [mm] from nozzle exit. On the same plane, some droplet variables will be numerically measured such as, droplet diameter, velocity and position for comparison purpose, using different approaches for turbulent dispersion. Also in the figure, it is shown a representative set of droplets colored in white, surrounding a grey liquid iso-surface equal to 0.01, which is the highest allowable value for droplet creation.

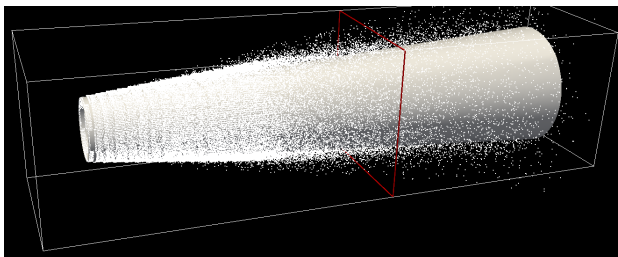


**Figure 2.** Measurement plane located at 5 diameters from the nozzle, represented by 4 red edges along with droplets colored as white dots.

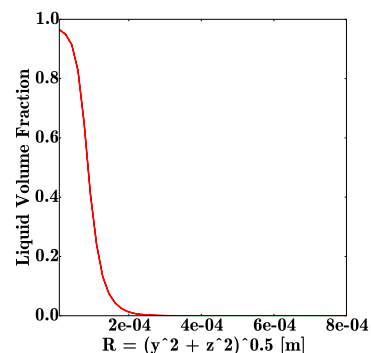


**Figure 3.** Euler liquid volume fraction at the red plane shown on the figure on the left.

On figure 3, liquid volume fraction is displayed averaged in time and radially in space at the mentioned plane. This liquid volume fraction radial profile will set the minimum radial distance from jet centerline, approximately 200 microns, to droplet formation.

Results are presented comparing three cases: a) SDE for particle trajectory with droplet injection velocity taken equal to Euler mixture velocity, b) SDE with droplet injection velocity taken equal to Euler mixture velocity plus an additional diffusive term undergoing a Wiener process with zero-mean random increment of standard deviation based on the local turbulent kinetic energy. And c) Direct Random Walk (DRW) model originally from OpenFOAM with droplet injection velocity taken equal to Euler mixture velocity. Results are brought in terms of *Probability density functions* (PDF) and its joint PDF for a pair of variables analysis. These PDF completely characterize the random process of the two-phase flow.

Probability density functions (PDF) for cases a), b), c) are shown in figure 4, on the left, center and right column, respectively. From top to bottom: PDF of droplet velocity, diameter and position for all the cases is displayed. On the left and center column, there is no appreciable difference between PDF velocity, diameter and position from case a) and b), which gives an indication of the nonexistent influence of adding a diffusive term for the velocity during at the injection. A difference can be distinguished by comparing the first two columns with the third one, specially for the PDF velocity, namely the shape of the PDF and averaged droplet velocities. It can be seen that both models can be approximated by log-normal and normal Gauss distribution, respectively, which is the logical expected result for the DRW model which uses the Gaussian diffusion process with zero-mean random increment of standard deviation based on the local turbulent kinetic energy. Moreover, a extended right tale can be seen on velocity PDF for DRW, which would wrongly give an impression of improvement over the SDE. On the other hand, the SDE by Langevin equation: 2, introduces additional terms based on the physics involved, such as the autocorrelation function, which relates the turbulence effect in a given time step, hence introducing some history of eddies in droplet trajectories.

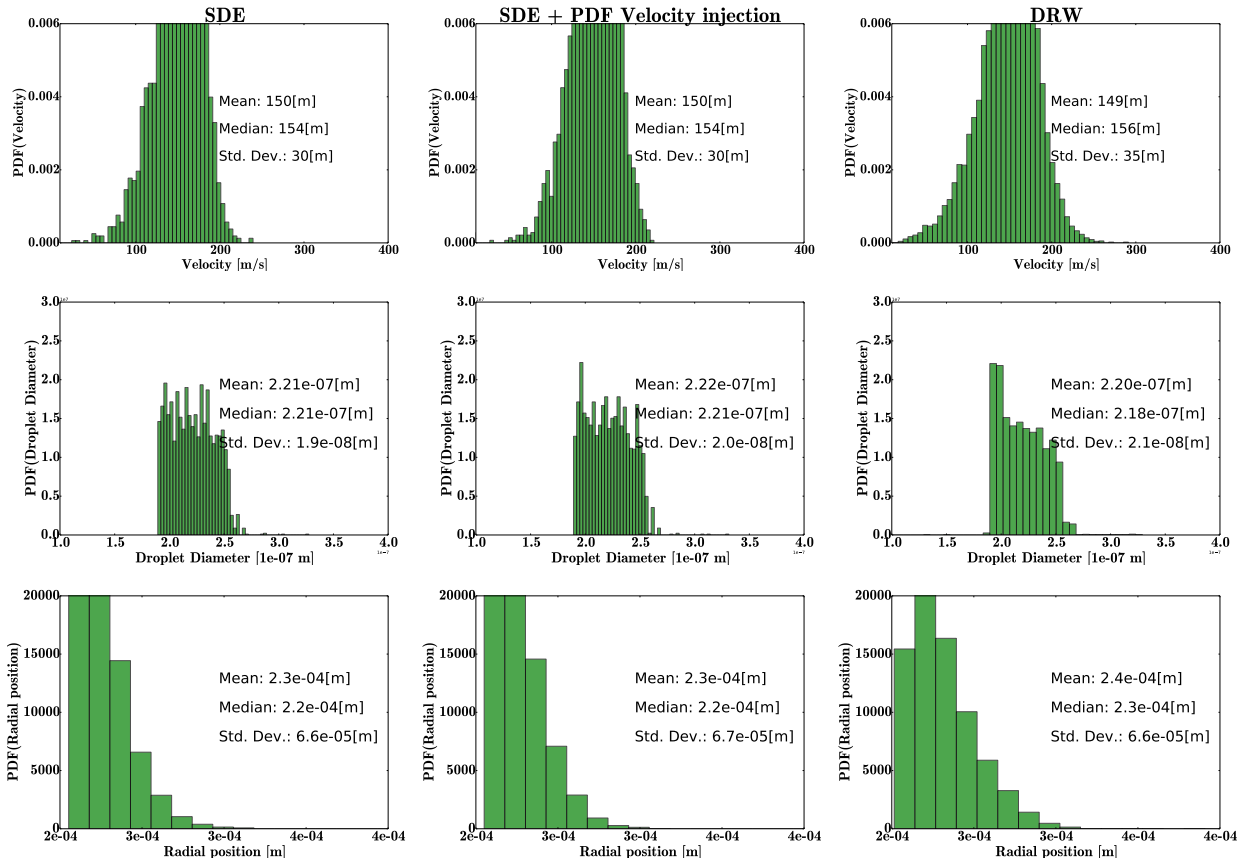


**Figure 4.** From top to bottom, PDF of droplet velocity, diameter and position at the plane, given by SDE, SDE with PDF velocity injection, and DRW model in OpenFOAM, respectively.

Finally looking at velocity magnitude probability, it was found no significance difference between the models. However, at the last row, some interesting findings can be drawn, specially compared to the experiments. It was found experimentally, droplets velocity as high as 150 m/s about a radial distance of 400 microns. Such values were in fact never obtainable using either model, as seen in bottom right image in figure 4 on the right, with almost zero probability of finding droplet beyond this point radially.

From top to bottom: Scatter plots, joint Probability density functions (PDF), and conditional PDF for cases a), b), c) are shown in figure 5, left, center and right, respectively. As the previous figures showed, little or not differences between case a) and b) is verified here as well. At the first row (the scatter plot), higher amount of droplets with higher velocity are displayed for DRW (up to 200 m/s), compared with both SDE models, especially in radial direction. However, based on the joint PDF on the second row, there is a wider velocity spectrum ranging from 150 to nearly 200 [m/s] with approximately equal probability for the SDE models compared to DRW. Regarding the occurrence probability of finding droplet close to 270 and 240 microns, on the third row, dots are the distributed samples of a joint PDF droplet velocity and radial position, where blue and red dots are the conditioned PDF velocity at radial position equal to  $\approx 240$  and 270 microns, respectively. Two main features can be deduced. 1) at 270 microns radially from the centerline, the expected velocity is approximately 150 m/s for all models. 2) At 240 microns radially from the centerline, the higher probability for DRW than SDE gives an indication of high droplet concentration around this radial position with approximately 90 m/s as expected velocity, on the contrary for the SDE with bigger variances and possible lower peak velocities, which are more in agreement with experimental findings as explained below.

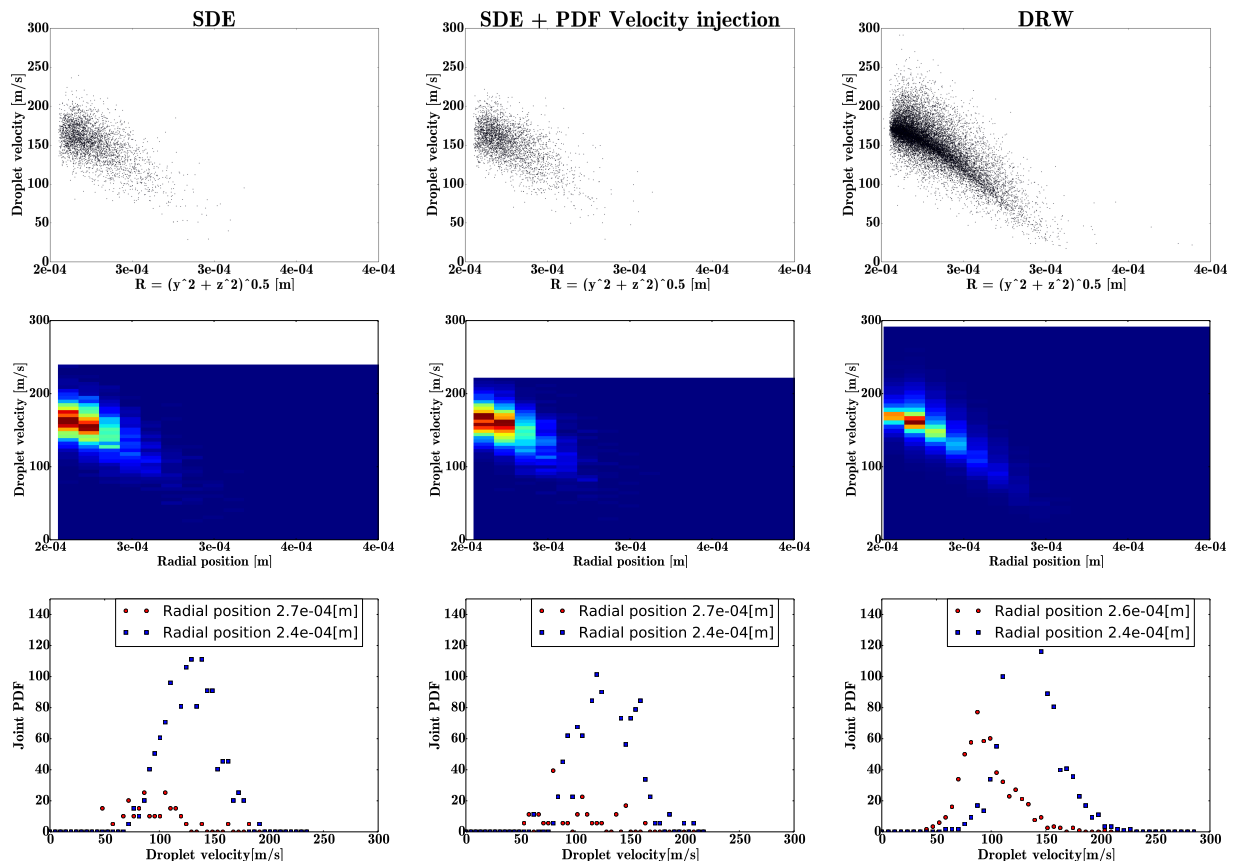


**Figure 5.** From top to bottom, scatter plot, joint PDF, and conditional PDF of droplet velocity at constant values of droplet position, given by SDE, SDE with PDF velocity injection, and DRW model in OpenFOAM, respectively.

Figure 6 exhibits the surface liquid velocity radially and time-averaged for experiments (black dots), DNS (blue line), and ELSA without Lagrange (continuous red line) [14, 19, 12]. Experimental results were taken using a kind of PTV measurements, based on structure detected techniques. Those velocities cannot be captured by the PTV instrument within the liquid jet core, as shown in the figure for radial distance lower than 200  $\mu\text{m}$ . Consequently,

in the absence of experimental dataset near the centerline of the liquid jet, DNS results were used. Therefore the available validation range is increased from the jet centerline up to 700  $\mu\text{m}$  approximately by combining both Experimental and DNS results. On one hand, it is noticeable after 200  $\mu\text{m}$  radially from the jet centerline ELSA results, without Lagrange (continuous red line), tend to underestimate the liquid velocity as compared to DNS and Experimental results. Such logical results arrive from the formation of tiny droplets beyond 200  $\mu\text{m}$ , thus unresolved scales become relevant as we move outward radially. On the other hand, adding the turbulent dispersion model developed by Langevin and implemented during this research for droplet velocities, enhanced ELSA results (orange and green lines, Langevin, and Langevin + Pdf-Inj, respectively), which clearly provides an improvement over the previous ELSA results by capturing until some extend those small droplets moving away from the centerline. Nonetheless, the difference observed between DNS and experiments are believed to be mainly due to RANS overestimated diffusiveness, thus with more or less influence on the space-averaged injection surface that might change the velocity momentum at which droplet are created. Finally, as shown previously, compared with Langevin modeling (orange line), there are no significance changes in droplet velocity distribution by adding a droplet velocity PDF at injection point (green line overlapping the orange one).

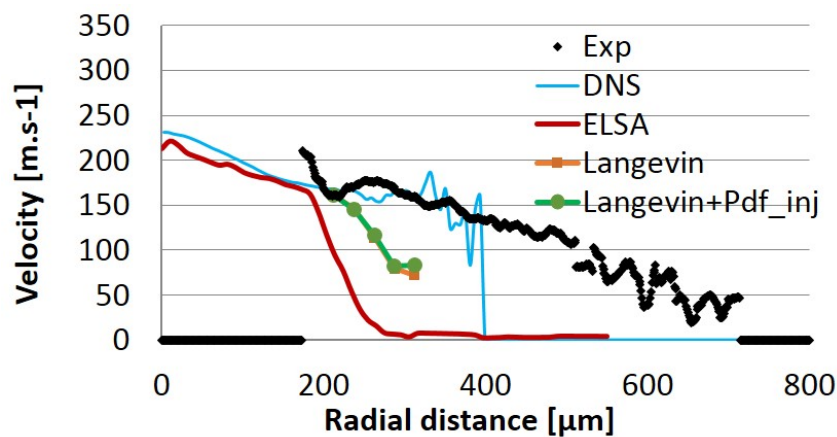


Figure 6. Radial interface velocity at 1500 [mm] from injector exit

### Summary and Conclusions

The one-way coupling between ELSA and Lagrange approach has been presented and tested. A new stochastic Lagrangian model based on the simplified Langevin model was implemented, which improves from the physical point of view the robustness of the turbulent dispersion for the droplet velocity undergoing Brownian motion, compared with the originally used Direct Random Walk (DRW) model, by means of well established DNS and experimental results. The droplet velocity injection distribution based on an additional diffusive term undergoing a Wiener process with zero-mean random increment of standard deviation based on the local turbulent kinetic energy, brought nonexistent statistical influence compared with cases without velocity distribution injection. The momentum transfer from the Euler part to droplets in SDE is higher, meaning there will be likely more particle with high velocities in outer radial regions from the centerline of the liquid jet than for the case of DRW, which is matchable with experimental results. This could be due to the turbulence memory added feature in SDE compared with DRW which helps in spreading them. It was found also DRW tends to concentrate droplets in regions not so far radially from the centerline.

### Acknowledgements

This work was fully supported by VINCI TECHNOLOGIES. Large part of results here reported have been obtained with CRIHAN (Centre Regional Informatique et d'Applications Numeriques de Normandie) and GENCI (IDRIS, Institut du developpement et des ressources en informatique scientifique) supercomputers. They are gratefully acknowledged.

## References

- [1] Antonio Andreini, Cosimo Bianchini, Stefano Puggelli, and FX Demoulin. Development of a turbulent liquid flux model for eulerian–eulerian multiphase flow simulations. *International Journal of Multiphase Flow*, 81:88–103, 2016.
- [2] Gregory Blokkeel, B Barbeau, and R Borghi. A 3d eulerian model to improve the primary breakup of atomizing jet. Technical report, SAE Technical Paper, 2003.
- [3] Romain Canu, Christophe Dumouchel, Benjamin Duret, Mohamed Essadki, Marc Massot, Thibault Ménard, Stefano Puggelli, Julien Reveillon, and François-Xavier Demoulin. Where does the drop size distribution come from? In *Ilass Europe. 28th european conference on Liquid Atomization and Spray Systems*, pages 605–612. Editorial Universitat Politècnica de València, 2017.
- [4] Renfeng Cao and Stephen B Pope. Numerical integration of stochastic differential equations: weak second-order mid-point scheme for application in the composition pdf method. *Journal of Computational Physics*, 185(1):194–212, 2003.
- [5] Jeremy Chesnel, Thibaut Menard, Julien Reveillon, and Francois-Xavier Demoulin. Subgrid analysis of liquid jet atomization. *Atomization and Sprays*, 21(1), 2011.
- [6] William T Coffey and Yuri P Kalmykov. *The Langevin equation: with applications to stochastic problems in physics, chemistry and electrical engineering*. World Scientific, 2004.
- [7] Clayton T Crowe. *Multiphase flow handbook*, volume 59. CRC press, 2005.
- [8] B Duret, J Reveillon, T Menard, and FX Demoulin. Improving primary atomization modeling through dns of two-phase flows. *International Journal of Multiphase Flow*, 55:130–137, 2013.
- [9] S Elghobashi. On predicting particle-laden turbulent flows. *Applied scientific research*, 52(4):309–329, 1994.
- [10] Zhi-Gang Feng and Efstathios E Michaelides. The immersed boundary-lattice boltzmann method for solving fluid–particles interaction problems. *Journal of Computational Physics*, 195(2):602–628, 2004.
- [11] OpenFOAM User Guide. Programmers guide. *JDT Core.*, retrieved from on Apr, 27(3), 2011.
- [12] Nicolas Hecht. *Simulation aux grandes échelles des écoulements liquide-gaz: application à l’atomisation*. PhD thesis, INSA de Rouen, 2016.
- [13] Romain Lebas, Thibault Menard, Pierre-Arnaud Beau, Alain Berlemont, and François-Xavier Demoulin. Numerical simulation of primary break-up and atomization: Dns and modelling study. *International Journal of Multiphase Flow*, 35(3):247–260, 2009.
- [14] Kamel Lounnaci, S Idlahcen, David Sedarsky, C Roze, Jean-Bernard Blaisot, and Francois-Xavier Demoulin. Image processing techniques for velocity, interface complexity, and droplet production measurement in the near-nozzle region of a diesel spray. *Atomization and Sprays*, 25(9), 2015.
- [15] Stephen B Pope. *Turbulent flows*, 2001.
- [16] Rajesh Reddy and Raja Banerjee. Direct simulations of liquid sheet break-up in planar gas blast atomization. *Atomization and Sprays*, 2017.
- [17] Mahdi Saeedipour, Stefan Pirker, Salar Bozorgi, and Simon Schneiderbauer. An eulerian–lagrangian hybrid model for the coarse-grid simulation of turbulent liquid jet breakup. *International Journal of Multiphase Flow*, 82:17–26, 2016.
- [18] Ariane Vallet and Roland Borghi. Modélisation eulerienne de l’atomisation d’un jet liquide. *Comptes Rendus de l’Académie des Sciences-Series IIB-Mechanics-Physics-Astronomy*, 327(10):1015–1020, 1999.
- [19] G Vaudor, T Ménard, W Aniszewski, M Doring, and A Berlemont. A consistent mass and momentum flux computation method for two phase flows. application to atomization process. *Computers & Fluids*, 152:204–216, 2017.